JOURNAL OF MATERIALS SCIENCE 22 (1987) 3446–3452

On the serrated yielding in Cu–14.1 at % Al polycrystals

SEI MIURA, ALI HAERIAN*, SATOSHI HASHIMOTO
Department of Engineering Science, Faculty of Engineering, Kyoto University, Kyoto-606, Japan

Cu–14.1 at % Al polycrystals with three different grain sizes (76,113 and 157 μm) have been tested for the Portevin–LeChatlier effect under various conditions of temperature (−196 to 200° C) and strain rate (2.78×10^{-5} to $5.56 \times 10^{-3}\,sec^{-1}$). In the above range of strain rate, serrated yielding was observed in the temperature range 60 to 160° C. The strain rate dependence of the onset of serrations is most probably due to the diffusion of vacancy–solute atom pairs, as indicated by the low value of the activation energy for migration (0.77 eV). The correlation governing the test variables at the onset of serrations appears to be: $\dot{\varepsilon} = (\text{const})\varepsilon_0^{2.2 \pm 0.2} \mu^{-0.87 \pm 0.03}$, where $\dot{\varepsilon}$, ε_0 and μ are strain rate, critical strain for the onset of serration and grain size, respectively. The onset of serrations is most probably due to dynamic strain ageing, although the possibility of short range ordering is not ruled out.

1. Introduction

Many solid solution alloys, both substitutional and interstitial, show serrated yielding after a smooth plastic flow within a certain range of test conditions, i.e. temperature and strain rate. This behaviour commonly called "repeated yielding" or "Portevin–LeChatelier Effect" has been the subject of intensive research since it was first observed by Portevin and LeChatelier in 1923 [1]. Different investigators have studied this effect in various alloy systems and have tried to explain the phenomenon by some suitable mechanism. Amongst these are the dynamic strain ageing model of Cottrell [2], the short range order effect proposed by Koppenaal and Fine [3], dislocation pile-up model of Korbel *et al.* [4, 5], and the cluster theory of Onodera *et. al* [6].

The dynamic strain ageing model is based on the interaction between solute atoms and moving dislocations enhanced by vacancies produced during deformation. Moving dislocations are repeatedly locked by solute atmosphere. When the rate of diffusion of solute atoms equals the speed of dislocation, dynamic strain ageing occurs.

The strengthening effect produced due to short range order can be calculated on the basis of the interaction between nearest neighbour shells and the constitution of the alloy [3]. Hence the change in yield stress at a serration may be compared to that caused by short range order strengthening.

The dislocation pile-up model and cluster theory mentioned above cannot be examined quantitatively; hence they will not be considered.

Other possible explanations for the Portevin–LeChatelier, P–L, effect are Suzuki locking [7] and Schoeck locking [8]. These possibilities are not ruled out and will be examined in the following sections.

2. Experimental procedure

Cu–14.1 at % Al prepared from 99.99% pure aluminium and 99.91% pure copper was drawn to a wire 1 mm in diameter. Test specimens 50 mm in length cut from this wire were annealed at 700° C for 20 min, straightened by rolling between two flat pieces of glass, reannealed in vacuum at 700, 800 and 950° C for 1 h and furnace cooled to room temperature to obtain various grain sizes.

Tensile tests were conducted at temperatures ranging from −196 to 200° C at strain rates between 2.78×10^{-5} and $5.56 \times 10^{-3}\,sec^{-1}$ using an Instron type machine. The gauge lengths of the specimens were 30 mm. Constant-temperature baths used for temperatures below 20° C were liquid nitrogen and alcohol cooled by liquid nitrogen. Water and silicon oil were used for baths of room temperature to 100° C and 100 to 200° C, respectively.

Grain size measurements and other measured parameters are presented in Table 1.

3. Theory

The dynamic strain ageing model of Cottrell [9] for the onset of serrated flow suggests that the critical velocity of moving dislocations below which the solute atmosphere forms around, and is dragged by the dislocation is

$$V_c = \frac{4D}{l} \tag{1}$$

where D is the diffusion coefficient of solute atoms at onset of serrations and l is the effective radius of the solute atmosphere. At this instant the critical strain rate is

$$\dot{\varepsilon} = b\varrho V_c = (4b\varrho/l)D \tag{2}$$

*On leave from Mechanical Engineering Department, Ferdowsi University, Mashhad, Iran.

0022–2461/87 $03.00 + .12 © *1987 Chapman and Hall Ltd.*

TABLE I The values of experimental results

Annealed temperature (°C)	Grain size (μm)	$\langle m + \beta \rangle$	Selected strain (%)	Activation energy Em (eV)	
				From $\dot{\varepsilon}T - 1/T$	From $\dot{\varepsilon} - 1/T$
			5	0.77	0.73
700	76	1.97	3	0.74	0.71
			1	0.82	0.78
			5	0.72	0.70
800	113	2.02	3	0.75	0.72
			1	0.84	0.81
			5	0.74	0.71
950	157	2.01	3	0.75	0.72
			1	0.79	0.75

where $\boldsymbol{b}$ is the Burgers vector, and ϱ is the mobile dislocation density. The diffusion coefficient of the solute atoms is given by Seitz [10] and Mott [11] as

$$D = a^2 v Z C_v \exp(-Em/kT) \quad (3)$$

where a is the lattice parameter, v Debye frequency, z the coordination number (12 for f c c structure), C_v the vacancy concentration, Em the effective activation energy for solute migration, k the Boltzman constant and T the temperature.

According to van Bueren [12]

$$C_v = B\varepsilon^m \quad (4)$$

where ε is the plastic strain and B and m are constants. ϱ is given by Conrad and Christ [13] as

$$\varrho = N\varepsilon^{\beta}\mu^{-n} \quad (5)$$

where n, N and β are constants and μ is the grain size. At the onset of serrations the critical strain ε_0 equals the plastic strain ε.

Substituting Equations 3, 4 and 5 into Equation 2 gives

$$\dot{\varepsilon} = (4a^2 \boldsymbol{b} N v z/l) B \varepsilon_0^{m+\beta} \mu^{-n} \exp(-Em/kT) \quad (6)$$

The term $Ba^2\boldsymbol{b}vz/l$ is constant, therefore for constant temperature and grain size

$$\dot{\varepsilon} = (\text{const})\varepsilon_0^{m+\beta} \quad (7)$$

which may be rewritten in logarithmic form as

$$\log \dot{\varepsilon} \propto (m + \beta) \log \varepsilon_0 \quad (8)$$

Hence, as it will be proved later, $(m + \beta)$ is temperature independent. If μ, ε_0 and $(m + \beta)$ are treated as constants, Equation 6 becomes

$$\ln\dot{\varepsilon} \propto -Em/kT \quad (9)$$

Therefore, it is possible to measure Em using Equation 9. The velocity of the moving solute atom V_i is given by the Einstein relation [14] as

$$V_i = \frac{DF}{kT} \quad (10)$$

where F is the interaction force between the dislocation and solute atom.

According to the Cottrell's model for serrated flow V_i must equal V_c. Substitution of Equation 10 in 2 gives

$$\dot{\varepsilon} = (Ba^2 \boldsymbol{b} N F v z/kT)\varepsilon_0^{m+\beta}\mu^{-n} \exp(-Em/kT) \quad (11)$$

where $Ba^2\boldsymbol{b}NFvz/k$ is constant. For constant temperature, grain size, $(m + \beta)$, μ and ε_0, Equation 11 reduces to

$$\ln(T\dot{\varepsilon}) \propto -Em/kT \quad (12)$$

Equation 12 is an alternative means for measuring activation energy Em.

4. Results

The stress–strain curves of the alloy at a strain rate of $2.78 \times 10^{-4}\,\text{sec}^{-1}$ at different deformation temperatures are presented in Fig. 1. As it is clear from these curves, the frequency of serrations increases with temperature, but at the same time they become less and less regular in shape.

Fig. 2 shows the effect of strain rate on the stress–strain curve. Here it is seen that increase in strain rate reduces the frequency of serrations, but they are more regular at higher strain rates. At any specific strain rate, the frequency of serrations increases with increasing strain.

4.1. Critical stress σ_0 and strain ε_0 for onset of serrations

The effect of strain rate and deformation temperature

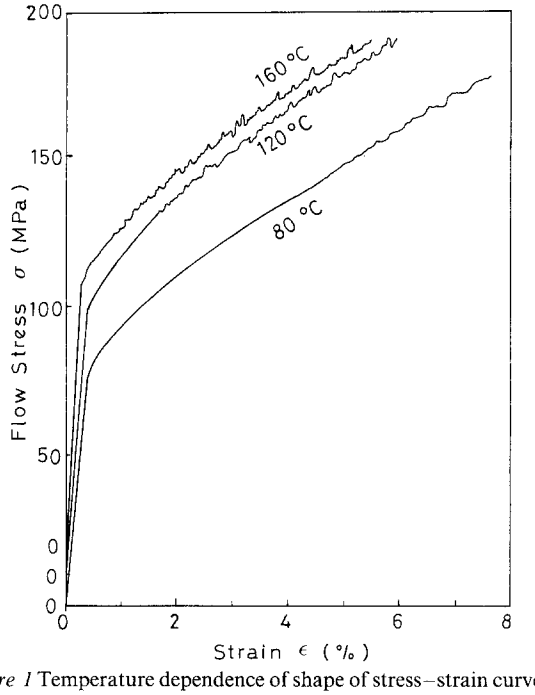

Figure 1 Temperature dependence of shape of stress–strain curve in Cu–14.1 at % Al alloys. Grain size 76 μm, strain rate $2.78 \times 10^{-4}\,\text{sec}^{-1}$.

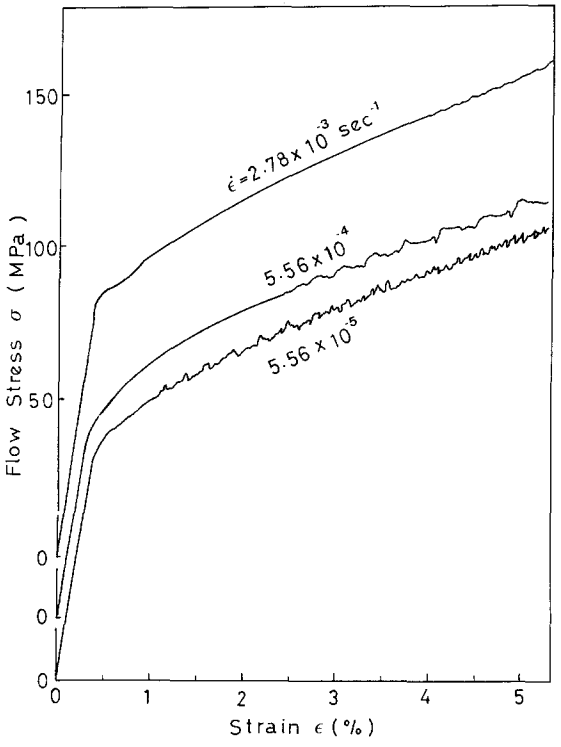

Figure 2 Strain rate dependence of shape of stress–strain curve in Cu–14.1 at % Al alloys. Grain size 76 μm, deformation temperature 120° C.

on ε_0 are shown in Figs 3 and 5, and on σ_0 in Figs 4 and 6. From these figures, it is clear that both critical stress and critical strain increase with increasing strain rate and decreasing deformation temperature. Both ε_0 and σ_0 show linear variation with strain rate on a log–log scale (figs 3 and 4).

Variation of ε_0 with grain size is shown in Fig. 5. This figure indicates that for any specific strain rate and at deformation temperature of 120° C, higher critical strains are expected for larger grain size material. Fig. 6 shows that the same tendency exists for deformation temperatures below 120° C, whereas for a deformation temperature of 140° C, there is a certain grain size for which ε_0 is minimal. Materials with larger or smaller grain size have higher critical strains.

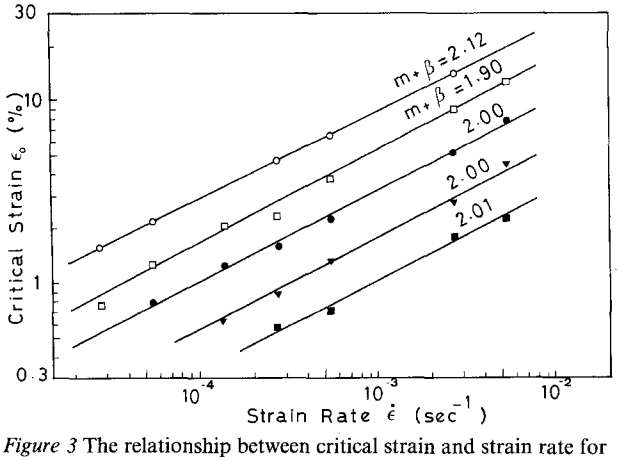

Figure 3 The relationship between critical strain and strain rate for selected temperature in Cu–14.1 at % Al alloys. Annealed at 950° C, grain size 157 μm, mean value $(m + \beta) = 2.01$. Deformation temperature (° C); (○) 80, (□) 100, (●) 120, (▼) 140, (■) 160.

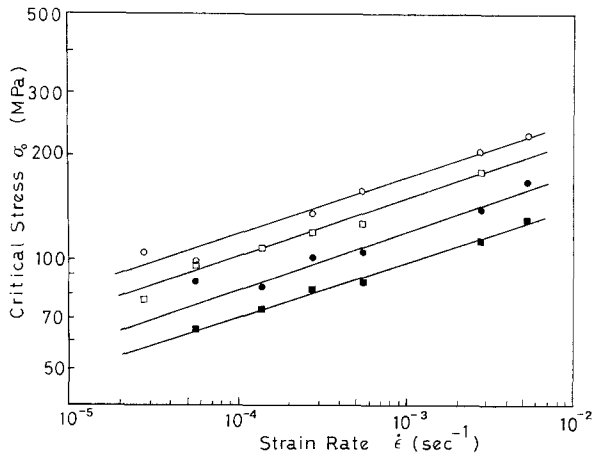

Figure 4 The relationship between critical stress and strain rate for selected temperature in Cu–14.1 at % Al alloys. Annealed at 950° C. Deformation temperature (° C); (○) 80, (□) 100, (●) 120, (■) 140.

4.2. Correlations between strain and vacancy concentration

Fig. 3 shows linear variation of log ε_0 with log $\dot{\varepsilon}$. This can be considered as a graphical representation of Equation 7 with the slope of the lines equal to $1/(m + \beta)$. The values of $(m + \beta)$ thus obtained for different grain sizes and deformation temperatures are presented in Table I. These values range from 1.8 to 2.3 with a mean value of 2.0 ± 0.2. Therefore Equation 7 becomes

$$\dot{\varepsilon} = (\text{const})\varepsilon_0^{2.0 \pm 0.2} \tag{13}$$

β, the exponent for dislocation density due to plastic strain is generally estimated for different metals to be ≈ 1.0. Hence Equation 4 becomes

$$C_v = B\varepsilon^{1.0 \pm 0.2} \tag{14}$$

4.3. Activation energy for vacancy migration

It has already been shown that $(m + \beta)$ is almost independent of temperature (Fig. 3 and Table I). Therefore, the activation energy for migration of vacancies, *Em*, may be calculated at a specific critical

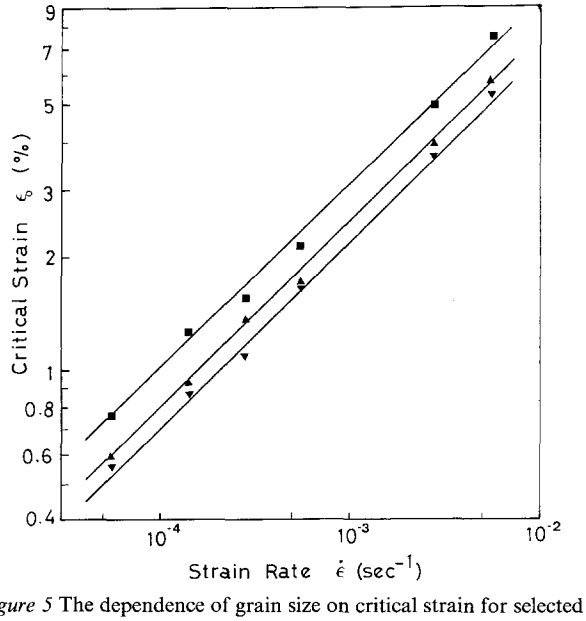

Figure 5 The dependence of grain size on critical strain for selected strain rate. Cu–14.1 at % Al. Deformation temperature, 120° C. Grain size (μm); (■) 76, (▲) 113, (▼) 157.

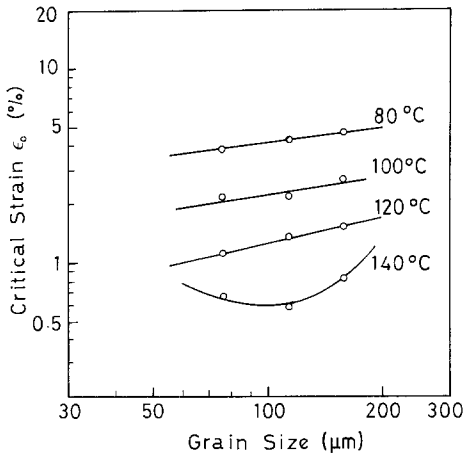

Figure 6 The relationship between critical strain and grain size at various deformation temperature in Cu–14.1 at % Al alloys. Strain rate $2.78 \times 10^{-4}\,sec^{-1}$.

strain. For example as shown in Fig. 7 for grain size of 157 μm, values of Em = 0.75, 0.72 and 0.71 eV (or 0.73 $\pm$ 0.02 eV) are obtained for strains of ε = 1, 3 and 5% respectively. Figures for other grain sizes are represented in Table I. Equation 11 for constant $(m + \beta)$ reduces to Equation 12. Hence, a plot of log $\dot{\varepsilon} T$ against $1/T$ also renders Em, which provides an alternative method for evaluation of this parameter. For example in Fig. 8 for grain size of 157 μm, values of Em = 0.79, 0.75 and 0.71 eV (or 0.765 $\pm$ 0.025 eV) are obtained for strains of 1, 3 and 5%, respectively.

4.4 Temperature dependence of work hardening

Fig. 9 shows the variation of flow stress with deformation temperature. In this figure the open squares correspond to conditions wherein no serrations were observed, while solid squares are indicative of observation of serrations. In the range about 0 to 30° C an

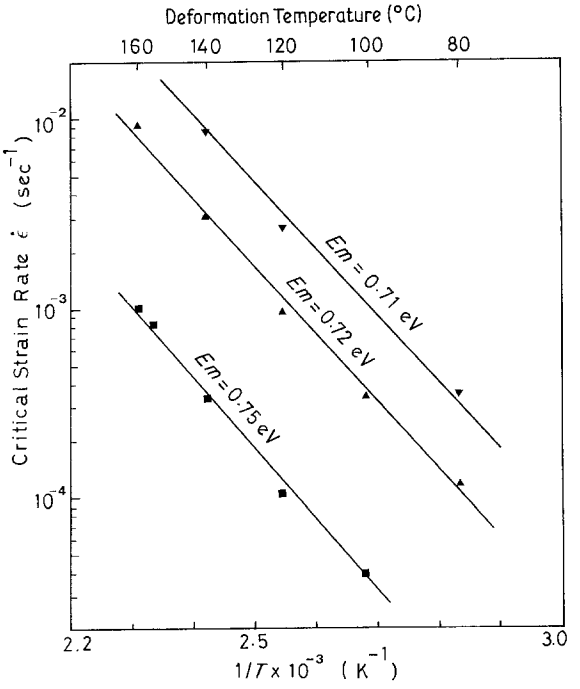

Figure 7 The relationship between critical strain rate and reciprocal temperature in order to determine activation energies for the process in Cu–14.1 at % Al alloys. Annealed at 950° C. Grain size 157 μm. (▼) ε = 5%, (▲) ε = 3%, (■) ε = 1%.

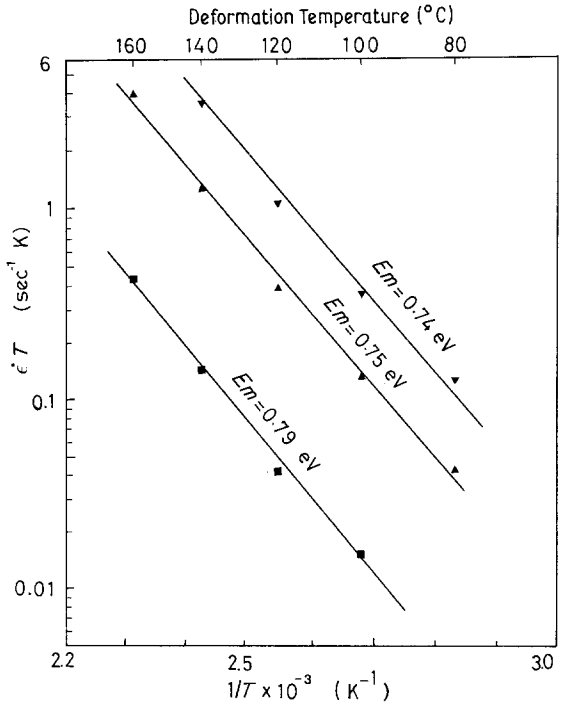

Figure 8 The relationship between critical strain rate times temperature and reciprocal temperature in order to determine activation energies for the process in Cu–14.1 at % Al alloys. Annealed at 950° C. Grain size = 157 μm. Strain; (▼) 5%, (▲) 3%, (■) 1%.

inverse effect of temperature on flow stress is observed, resulting in higher stress levels than extrapolated values for higher temperatures. Apart from this behaviour in the range 0 to 30° C, ε_0 decreases with increasing deformation temperature.

5. Discussion

5.1. Serrations

According to Cottrell [2], serrations occur when the velocity of moving dislocations V_c equals the solute atom drift velocity. Equation 3 shows that for constant temperature, diffusion coefficient D is only a function of the vacancy concentration C_v, which in turn is only dependent on strain ε (Equation 4). i.e.

$$D \propto f_1(C_v) \propto f_2(\varepsilon) \tag{15}$$

Therefore, increasing $\dot{\varepsilon}$ must increase D, that is ε is increased to produce more vacancies (Fig. 3).

Equation 6 for constant strain rate gives

$$\dot{\varepsilon}\ (= \text{const}) = (\text{const})\varepsilon_0^{m+\beta} \exp(-Em/kT) \tag{16}$$

Hence, the exponent term increases with increasing T with a consequence of reduction in ε_0 (Fig. 5). It is clear that the present results qualitatively approve Cottrell's model.

TABLE II The values of index $(m + \beta)$

Specimen	$m + \beta$	Investigators
Cu–Sn alloy	1.9	Vöringer *et al.* [15]
Cu–1 ~ 7 at % Sn	2.2 $\pm$ 0.1	Russell [16]
Cu–30 wt % Zn	1.9	Charnock [17]
Cu–20 ~ 35 wt % Zn	1.9 ~ 3.7	Munz *et al.* [18]
Cu–14.1 at % Al	2.0 $\pm$ 0.2	Present work

TABLE III The values of index β

Specimen	β	Investigators
Cu alloy	1.2	Lomer *et al.* [19]
Cu–3.2 at % Sn	1.17	Ham *et al.* [20]
Pure Cu	1.0	Baily [21]
Ag–6.3 Al	1.14–1.15	Hashimoto and Miura [22]
Cu–27.8% Zn	1.00 ± 0.02	Miura and Matsuba [23]

5.2. Dependence of serrations on ε_0 and $\dot{\varepsilon}$

The relationship between ε_0 and $\dot{\varepsilon}$ for serrated flow is shown in Fig. 3 (Equation 13). The value $(m + \beta) = 2.0 \pm 0.2$ is comparable to those obtained by other investigators for different alloys (Table II).

Table III shows values of β for several fcc substitutional solid solutions. Assuming $\beta = 1$, gives $m = 1.0 \pm 0.2$ (Equation 14) which is smaller than the value 1.3 for α-brass reported by Bolling [24]. However, Charnock [17] has considered $m = 1.3$ an overestimation.

5.3. Effect of grain size on serrations

For constant T, Equations 6 and 11 reduce to

$$\dot{\varepsilon} = (\text{const})\ \varepsilon_0^{m+\beta} \mu^{-n} \tag{17}$$

As mentioned before, $(m + \beta)$ is independent of grain size, hence for constant ε_0, Equation 17 becomes

$$\dot{\varepsilon} = (\text{const})\ \mu^{-n} \tag{18}$$

Equation 17 can be rewritten as

$$\varepsilon_0 = (\text{const})\ \dot{\varepsilon}^{1/(m+\beta)}\ \mu^{n/(m+\beta)} \tag{19}$$

which for constant $\dot{\varepsilon}$ becomes

$$\varepsilon_0 = (\text{const})\ \mu^{n/(m+\beta)} \tag{20}$$

n can be estimated from Fig. 10 (or Equation 18), or Fig. 11 (or Equation 20). The values of n thus estimated are 0.87 ± 0.03 and 0.89 ± 0.03, respectively, which are close enough within experimental error. However, the former value ($n = 0.87$) is more reliable, as the error associated with $(m + \beta)$ is excluded. Hence Equation 17 becomes

$$\dot{\varepsilon} = (\text{const})\ \varepsilon_0^{2.0\pm0.2}\ \mu^{-0.87\pm0.03} \tag{21}$$

The values of n estimated in present work are compared with those obtained by other methods in Table IV.

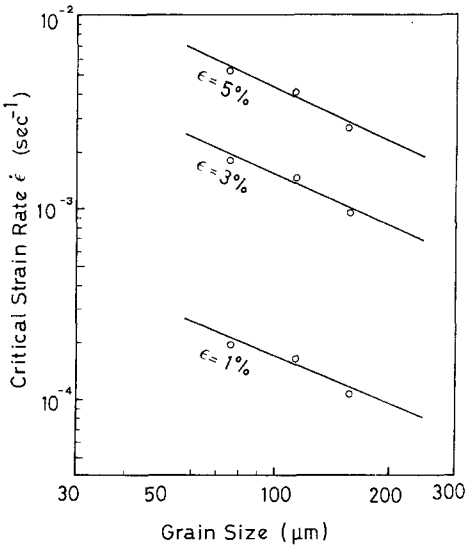

Figure 10 The relationship between the critical strain rate and grain size for the constant critical strain at 120° C in Cu–14.1 at % Al alloys.

5.4. Work hardening coefficient

Generally flow stress is expressed in terms of strain as

$$\sigma = A\varepsilon^p \tag{22}$$

where p, the work hardening exponent has a positive value. Equation 22 can be rewritten as

$$\varepsilon = A'\sigma^{1/p} \tag{23}$$

In the above two equations A and A' are constants. Substituting Equation 23 in Equation 7 for the condition $\varepsilon = \varepsilon_0$ and $\sigma = \sigma_0$ gives

$$\sigma = (\text{const})\ \varepsilon^{p/(m+\beta)} \tag{24}$$

The exponent $p/(m + \beta)$ is the slope of the plot of log $\dot{\varepsilon}$ against log σ. Knowing $m + \beta$, p is calculated. From Fig. 5, $p = 0.33$ is obtained. Hence Equation 22 becomes

$$\sigma = A\varepsilon^{0.33} \tag{25}$$

5.5. Activation energy for vacancy migration

From the two sets of values for *Em* in Table I, the first

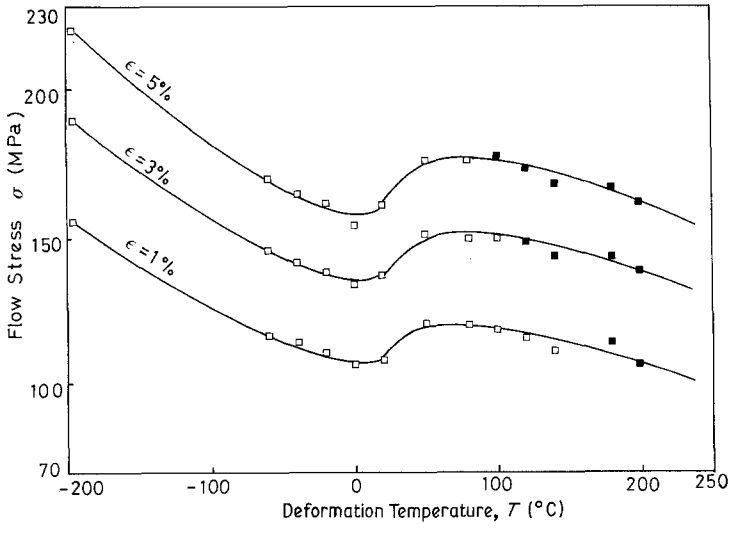

Figure 9 The dependence of deformation temperature on flow stress for selected strain at the strain rate of 5.56×10^{-4} sec^{-1} in Cu–14.1 at % Al alloys. (□) no serrations, (■) observed serrations. Annealed at 800° C. Strain rate $\dot{\varepsilon} = 5.56 \times 10^{-4}$ sec^{-1}.

TABLE IV The values of index n

Specimen	n	References	Methods
Cu	0.5	Conrad *et al.* [13]	Resistivity measurement
Fe	0.5	Keh *et al.* [25]	TEM
Cu–30 at % Zn	1.0	Charnock [17]	TEM
Cu–14.1 at % Al	0.87 ± 0.03	Present work	Dynamic strain ageing

set (determined from log $\dot{\varepsilon}$ against $1/T$, Fig. 7) are in the order of 0.03 ~ 0.04 eV higher than the second set. This discrepancy is not unexpected, as two different approaches are used. The first set of data is on the basis of the effective radius of solute atmosphere, whereas the second set is based on the interaction between dislocations and solute atoms (diffusion). The second approach is preferred, and as *Em* is independent of grain size, the value 0.77 eV is used for further work.

Values of *Em* for pure copper and copper alloys reported by various investigators are listed in Table V. The values quoted from Koppenaal and Fine [3] are from static strain ageing measurements for different ageing times. Therefore, *Em* values corresponding to lower ageing times can be compared with the *Em* for dynamic strain ageing. The value 0.77 eV obtained in the present work is close to the lower limits of *Em* values given by Koppenaal and Fine.

There are not many reports regarding the measurement of the binding energy between solute atoms and vacancies in copper. The present work provides a means for assessment of this parameter through measurement of activation energy for migration of vacancies in pure metal, *Em*.

If a vacancy and a solute atom migrate as a pair

$$Em = E_{IV}^{m} - E^{B} \quad (26)$$

But, if a vacancy migrates by breaking away from the solute atom

$$Em = E_{IV}^{m} + E^{B} \quad (27)$$

According to the data presented in Table V, the migration energy in pure copper is greater than 1.0 eV. The fact that E_{IV}^{m} is greater than *Em* indicates that migration takes place as a vacancy–solute atom pair.

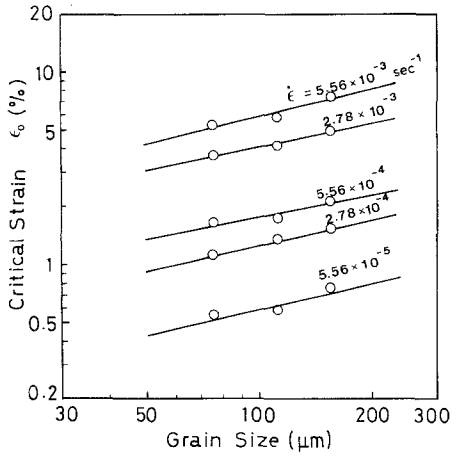

Figure 11 The relationship between the critical strain and grain size for the constant critical strain rate at 120° C in Cu–14.1 at % Al alloys.

Therefore, the binding energy is

$$E^{B} = 1.00 - 0.77 = 0.23\,\text{eV} \quad (28)$$

5.6. Mechanisms of serrated yielding

As mentioned in Section 1, the mechanisms proposed for serrated yielding are the Cottrell effect [2], Suzuki locking [31], short range ordering [3] and Schoeck locking [8] (stress induced short range order).

Amongst the above mechanisms, the first three depend on the diffusion of solute atoms, but the last one, Schoeck locking, is assisted by stress, and thermal diffusion is not the necessary condition for its occurrence. Therefore, this possibility is rather weak.

Howie and Swann [7] did not observe the precipitates indicative of Suzuki locking in Cu–Al alloys. Hence Suzuki locking is not considered as a strong possibility.

Occurrence of short range order in Cu–Al alloys has been confirmed by X-ray scattering [32]. Cottrell [33] has mentioned the possibility of short range order being responsible for yielding in these alloys. Koppenaal and Fine [3] have shown that both a yield point effect and strain ageing may be attributed to short range ordering.

Although, the present results confirm the Cottrell model as a strong possibility for the onset of serrations, the mechanism responsible for their continuation is not as clear. The fact that Cu–Al alloys have extended dislocations and stacking faults are produced between them makes the Cottrell model less favoured.

5.7. Temperature dependence of work hardening

The increase in critical strain due to increase in strain rate observed in Fig. 10 may be attributed to the locking of dislocations by solute atoms. Nevertheless, this condition is necessary but not sufficient. According to Koppenaal and Fine increasing T or decreasing $\dot{\varepsilon}$ enhances diffusion, so that the degree of ordering increases. Hence increase in stress is not only due to the locking of dislocations by solute atoms, but may be due to short range ordering as well.

6. Conclusions

1. Cu–14.1 at % Al shows serrated yielding in the temperature range 60 to 160° C and at strain rates between 2.78×10^{-5} and $5.56 \times 10^{-3}\,\text{sec}^{-1}$. The strain rate dependence is due to the diffusion of vacancy–solute atom pairs.

2. The index $(m + \beta)$ is independent of grain size and is estimated to be 2.0 ± 0.2.

3. Activation energy of vacancy migration which is independent of grain size is estimated to be 0.77 eV.

TABLE V The values of activation energy *Em* (eV)

Specimen	*Em* (eV)	References	Methods
Cu–1 ~ 7 at % Sn	0.79 ± 0.05	Russell [16]	Dynamic strain ageing
Cu–4 wt % Sn	0.71 ± 0.05	Russell *et al.* [26]	Static strain ageing
Cu–20 ~ 35 wt % Zn	0.47 ~ 0.70	Munz *et al.* [18]	Dynamic strain ageing
Cu–14 at % Al	0.67 ~ 1.13	Koppenaal *et al.* [3]	Static strain ageing
Pure Cu	0.88 ± 0.13	Simmons [27]	Thermal equilibrium
Pure Cu	1.3	Airoldi *et al.* [28]	Quenching
Pure Cu	0.7	Kimura *et al.* [29]	Quenching
Pure Cu	1.0	Schüle *et al.* [30]	Quenching, deformation
Cu–14.1 at % Al	0.76 ~ 0.78	Present work	Dynamic strain ageing

Therefore the diffusion of vacancy–solute atom pairs seems to be the operative mechanism.

4. The interrelation between $\dot{\varepsilon}$, ε_0 and μ at the onset of serrations is $\dot{\varepsilon} = (\text{const})\,\varepsilon_0^{2.0\pm0.2}\mu^{-0.87\pm0.03}$

5. Short range order assisted by diffusion and the Cottrell effect seem to be the two possible operative mechanisms.

Acknowledgements

The authors wish to thank Mr T. Une for valuable assistance in the experimental work.

References

1. A. PORTEVIN and F. LE CHATELIER, *C. R. Acad. Sci.* **176** (1923) 507.
2. A. H. COTTRELL, *Phil. Mag.* **44** (1953) 829.
3. T. J. KOPPENAAL and H. E. FINE, *Trans. AIME* **221** (1961) 1178.
4. A. KORBEL, *Scripta Met.* **8** (1974) 609.
5. A. KORBEL, J. ZASADZINSKI and Z. SIEKLUCKA, *Acta Met.* **24** (1976) 919.
6. R. ONODERA, T. ISHIBASHI, M. KOGA and M. SHIMIZU, *ibid.* **31** (1983) 535.
7. A. HOWIE and P. R. SWANN, *Phil. Mag.* **6** (1961) 1215.
8. G. SCHOECK, *Phys. Rev.* **102** (1956) 1459.
9. A. H. COTTRELL, "Dislocation and Plastic Flow in Crystals" (Clarendon, Oxford, 1953) p. 136.
10. F. SEITZ, *Advance. Phys.* **1** (1952) 43.
11. N. F. MOTT, *Phil. Mag.* **43** (1952) 1151; *ibid.* **44** (1953) 187, 742.
12. H. G. VAN BUEREN, *Z. Metalldke.* **46** (1955) 272; *Acta Met.* **3** (1955) 519.
13. H. CONRAD and B. CHRIST, "Recovery and Recrystallizations of Metals" (1963) p. 124.
14. See for example, J. FRIEDEL, "Dislocations" (Pergamon Press, Oxford, 1964) p. 84.
15. V. O. VÖHRINGER and E. MACHERAUCH, *Z. Metallkde.* **58** (1967) 317.
16. B. RUSSELL, *Phil. Mag.* **8** (1963) 615.
17. W. CHARNOCK, *ibid.* **18** (1968) 89.
18. D. MUNZ and E. MACHERAUCH, *Z. Metallkde.* **57** (1966) 552.
19. J. N. LOMER and H. M. ROSENBERG, *Phil. Mag.* **4** (1959) 467.
20. R. K. HAM and D. JAFFREY, *ibid.* **1** (1967) 247.
21. J. E. BAILY, *ibid.* **8** (1963) 223.
22. S. HASHIMOTO and S. MIURA, *Mem. Fac. Eng. Kyoto Univ.* **48** (1986) 30.
23. S. MIURA and H. MATSUBA, The Science and Engineering Review of Doshisha University **20** (1979) 8.
24. G. F. BOLLING, *Phil. Mag.* **4** (1959) 537.
25. A. S. KEH and S. WEISSMAN, "Electron Microscopy and the Strength of Crystals" (1961) p. 231.
26. B. RUSSELL and P. VELA, *Phil. Mag.* **8** (1963) 172.
27. R. O. SIMMONS, *J. Phys. Soc. Jpn* **18** (Suppl.) (1963) 172.
28. G. AIROLDI, G. L. BACCELLA and E. GERMAGNOLI, *Phys. Rev. Lett.* **2** (1959) 145.
29. H. KIMURA, R. MADDIN and D. KUHLMANN-WILSDORF, *Acta Met.* **7** (1959) 145.
30. W. SCHÜLE, A. SEEGER, F. RAMSTEINER, D. SCHULEMACHER and K. KING, *Z. Naturforsch.* **15a** (1961) 323.
31. H. SUZUKI, "Dislocations and Mechanical Properties of Crystals" (John Wiley, New York, 1957) p. 361.
32. C. R. HOUSKA and B. L. AVERBACH, *J. Appl. Phys.* **30** (1959) 1525.
33. A. H. COTTRELL, "Relation of Properties to Microstructure" (ASM, Cleveland, 1954) p. 131.

Received 29 August 1986
and accepted 10 February 1987